Stem Cell Research (2013) 11, 951–964

Available online at www.sciencedirect.com

SciVerse ScienceDirect

www.elsevier.com/locate/scr

Cell biological effects of mechanical stimulations generated by focused extracorporeal shock wave applications on cultured human bone marrow stromal cells

Frank Suhr[a,1,2], Yvonne Delhasse[a,1,3], Gerd Bungartz[a,b,4,5], Annette Schmidt[a,c,1,6], Kurt Pfannkuche[d,7,8], Wilhelm Bloch[a,*,9]

[a] Institute of Cardiovascular Research and Sport Medicine, Department of Molecular and Cellular Sport Medicine, German Sport University Cologne, Cologne, Germany
[b] Harvard Stem Cell Institute, Harvard University, Boston, MA, USA
[c] Bundeswehr Institute of Pharmacology and Toxicology, Munich, Germany
[d] Institute of Neurophysiology, Medical School of University of Cologne, Cologne, Germany

Received 7 August 2012; received in revised form 20 March 2013; accepted 18 May 2013
Available online 29 May 2013

Abstract Human bone marrow stromal cells (hBMSCs) bear tremendous clinical potential due to their immunomodulatory properties in transplantation settings and their contribution to tissue regeneration. In fact, they are among the most promising types of stem-like cells for therapeutic applications and are the subject of intense research. However, the clinical use of hBMSCs has been confounded by limitations in their availability; they are scarce cells cumbersome to isolate and purify. Additionally, they are difficult to target to the site of injury in regeneration experiments. In order to combat these limitations, focused extracorporeal shock waves (fESW, 0.2/0.3 mJ * mm^{-2}) were applied to purified, cultured hBMSCs. fESW (0.2 mJ * mm^{-2}) stimulations were found to increase hBMSCs' growth rate ($p < 0.05$), proliferation ($p < 0.05$), migration, cell tracking and wound healing ($p < 0.05$, respectively), as well as to reduce the rate of apoptosis activation ($p < 0.05$). The increase in hBMSC migration behavior was found to be mediated by active remodeling of the actin cytoskeleton as indicated by increased directed stress fiber formations ($p < 0.05$). Furthermore,

* Corresponding author at: Institute of Cardiovascular Research and Sport Medicine, Department of Molecular and Cellular Sport Medicine, German Sport University Cologne, Am Sportpark Müngersdorf 6, 50933 Cologne, Germany. Tel.: +49 221 4982 5440, +49 221 4982 5390; fax: +49 221 4982 8370.
E-mail addresses: Suhr@dshs-koeln.de (F. Suhr), Yvonnedelhasse@gmx.de (Y. Delhasse), G.Bungartz@dshs-koeln.de (G. Bungartz), Annette2Schmidt@bundeswehr.org (A. Schmidt), akp59@uni-koeln.de (K. Pfannkuche), W.Bloch@dshs-koeln.de (W. Bloch).
[1] Am Sportpark Muengersdorf 6, 50933 Cologne, Germany. Tel.: +49 221 4982 5440; fax: +49 221 4982 8370.
[2] Conception and design of the study, assembly of data, data analysis and interpretation, manuscript writing.
[3] Conception and design, collection of data, data analysis.
[4] Present address: Am Sportpark Muengersdorf 6, 50933 Cologne, Germany. Tel.: +49 221 4982 5440; fax: +49 221 4982 8370.
[5] Data analysis, manuscript writing.
[6] Conception and design of the study.
[7] Robert-Koch-Straße 39, 50931 Cologne, Germany. Tel.: +49 221 478 6960; fax: +49 221 478 6965.
[8] Manuscript revision for critical intellectual impact.
[9] Financial support, manuscript revision for critical intellectual impact, final approval of the manuscript.

1873-5061/$ - see front matter
http://dx.doi.org/10.1016/j.scr.2013.05.010

hBMSCs maintain their differentiation potentials after fESW treatment, whereas 0.2 mJ * mm^{-2} is the most effective application. In conclusion, our results establish first-timely that hBMSCs' behavior can be modified and optimized in response to defined mechanical stimulation. These findings appear particularly promising as they suggest that mechanical stress preconditions hBMSCs for improved therapeutic performance without genetic manipulations and that mechanically preconditioned hBMSCs will be advantageous for hBMSC-based tissue regeneration. Therefore, this approach opens the door for exploiting the full potential of these cells in regenerative medicine.

Introduction

Human bone marrow stromal cells (hBMSCs) are characterized by their capability to differentiate into various mesenchymal tissues, including adipocytes, chondrocytes and osteocytes (Ciapetti et al., 2006; Kuznetsov et al., 1997a; Meinel et al., 2004; Pittenger et al., 1999; Tondreau et al., 2004). hBMSCs are a promising tool for the field of regenerative medicine for several reasons; they can be cultured ex vivo, have endogenous activation potential (Jiang et al., 2002; Pittenger et al., 1999), can be systemically delivered or undergo allogeneic transplantation (Krause et al., 2007; Wolf et al., 2009) and have a high self-renewal potential (English et al., 2010; Kolf et al., 2007; Nombela-Arrieta et al., 2011; Song et al., 2006; Zaragosi et al., 2006). Their immunosuppressive properties make them a promising tool to counter complications arising from graft versus host rejections in transplantation settings of cells other than hBMSCs (English et al., 2010; Prockop, 2009). It should be noted that the transplantations of BMSCs have not been highly successful, yet, in order to cure disease tissue, as BMSCs disappear within a short period of time after transplantation. However, a myriad of research is still geared towards utilizing their differentiation potential for tissue engineering approaches, particularly for cartilage and bone regeneration (Nombela-Arrieta et al., 2011) indicating the unraveled potential of BMSCs in tissue regeneration.

How hBMSCs exert their beneficial effects in tissue regeneration is, however, less clear. It was first hypothesized that BMSCs engraft directly into the degenerative tissue and differentiate into the respective cell type (Mahmood et al., 2003; Murphy et al., 2003). However, there is accumulating evidence in favor of a second hypothesis postulating that BMSCs predominantly contribute to tissue regeneration by their capability to secrete a variety of trophic factors contributing to paracrine effects in tissue repair (Gnecchi et al., 2005; Haynesworth et al., 1996; Ladage et al., 2007; Mirotsou et al., 2007) rather than tissue-specific differentiation (Prockop, 2009). Regardless of how BMSCs unfold their remarkable healing properties, it has been demonstrated in different studies that only a low percentage of transplanted hBMSCs reaches the targeted disease area (Hofmann et al., 2005) and that after a few days, only a small amount (2–6%) persists in the affected tissue (Hofmann et al., 2005; Kolf et al., 2007). In addition to the limitation of the presence of BMSCs at the site of injury, certain proportions of these cells need to display proliferative and apoptotic, as well as migratory, behaviors in order to mediate tissue repair (Li and Jiang, 2011; Schmidt et al., 2006). Thus, the therapeutic success of using hBMSCs in tissue regeneration has been limited and falls far behind their potential.

In order to increase the efficiency of targeting hBMSCs to the disease area and to promote their beneficial cellular response at those desired targets for therapeutic use, novel strategies avoiding genetic manipulation are needed (Karp and Leng Teo, 2009; Peterson et al., 2011; Schumann et al., 2006; Yan et al., 2011) to precondition BMSCs (Ghanem et al., 2009). Extracorporeal shock waves (ESW) are transient pressure fluctuations that propagate 3-dimensionally and that are widely applied in the context of therapeutic mechanotransduction with a high success of increased tissue regeneration (Nishida et al., 2004; van der Jagt et al., 2011, 2013). Two major types of ESW are used in medical therapies, focused and radial ESW, whereas the former ESW type reflects high-peak pressure amplitudes and the majority of energy flux is concentrated on a small focus (Chang et al., 2012). These data show that focused ESW (fESW) types might be a suitable tool for preconditioning hBMSCs in order to improve their therapeutic potentials.

It is known that the expression of genes involved in differentiation pathways of hBMSCs can be influenced by mechanical stimuli (Friedl et al., 2007). Different groups have shown that ESW offer great beneficial potential in the treatment of patients suffering from different conditions, including injured bone, cartilage and cardiac tissue (Nishida et al., 2004; Wang et al., 2003). Unfortunately, the mechanistic foundation for these improvements has not been addressed in these studies and the identity of cellular contributors has not been confirmed. In this context, no knowledge exists concerning the potential effects of ESW application on cell biological properties of hBMSCs, such as proliferation and migration, that are crucial for successful medical BMSC-based therapies (Li and Jiang, 2011). Additionally, it remains unclear whether hBMSCs maintain their full differentiation potentials after treatment with mechanical stimuli.

To address the unresolved, but highly significant question of whether hBMSCs' behavior can be manipulated by ESW application and whether those manipulations depend on energy and/or timing of ESW application as well as whether hBMSCs maintain their full differentiation potentials after ESW treatment, the present study hypothesized (I) that ESW applications induce cell biological effects on purified cultured hBMSCs that prove beneficial for tissue regeneration, (II) that the cell biological processes are dependent on the dose of ESW application and (III) that hBMSCs maintain their full differentiation potentials after ESW applications. The results clearly demonstrate that ESW promote biological processes in hBMSCs, including increased proliferation, survival and migration, which are described to prove beneficial for tissue regeneration. Additionally, ESW do not disturb hBMSCs' differentiation potentials. Therefore, the presented observations demonstrate that ESW stimulations of a defined nature are a dynamic approach to manipulate hBMSC behavior in vitro in order to exploit their full regenerative capacity in vivo. Furthermore,

the benefits of ESW application are obtained without any manipulation prohibitive to immediate therapeutic application.

Materials and methods

hBMSC isolation and culture

Adult hBMSCs were isolated from the bone marrow of human femoral heads from patients receiving hip joint replacements. The average age of the patients was 73 ± 7.4 years. Only material that tested negative for HIV and hepatitis was accepted. After abrading the marrow of the femoral head and filtering the marrow with PBS up to a volume of 50 mL, a density gradient centrifugation was performed. The fraction containing hBMSCs was purified as described recently (Steingen et al., 2008). Cells were cultured in alpha modifications of Eagle's Medium (alpha-MEM, PAA with Glutamine, without Nucleosides, Cölbe, Germany) supplemented with 20% FCS (Biowest, Nuaille, France). The medium was changed the first time after two days of culture. The cells were used up to passage 3 and plated at a density of 2000 cells $*$ cm^{-2} for culturing purposes (Schmidt et al., 2006). hBMSCs were passaged by Accutase™ with an optimal confluence of approximately 80%. The study was authorized by the ethics commission of the Medical School of the University Cologne and was in line with the declaration of Helsinki.

hBMSCs characterization

Briefly, hBMSCs were characterized using FACS analysis as described by Steingen (2008). Freshly isolated hBMScs were plated with a density of 1000 cells$*$cm^{-2} (adipogenic and osteogenic differentiation) or 2000 cells $*$ cm^{-2} (chondrogenic differentiation), respectively, and were characterized using a colony-forming unit-fibroblast (CFU-F) as described earlier (Friedenstein et al., 1966, 1976). Thereby, it should be noted that populations of human marrow CFU-Fs are heterogeneous with respect to their differentiation capacity (Kuznetsov et al., 1997b; Sacchetti et al., 2007). The identity of hBMSCs was confirmed by established methods in our lab culturing the hBMSCs under conditions favorable for adipogenic [basic medium: alpha-MEM; 2 mM L-glutamine (Sigma-Aldrich, Munich, Germany), 60 μM indomethacin (Sigma-Aldrich, Munich, Germany), 1 μM dexamethasone (Sigma-Aldrich, Munich, Germany), 0.5% antibiotics-antimycotics (Invitrogen, Karlsruhe, Germany), 5 μg $*$ mL^{-1} insulin (Sigma-Aldrich, Munich, Germany), 15% FCS (Biowest, Nuaille, France)], chondrogenic [basic medium: D-MEM; 2 mM L-glutamine (Sigma-Aldrich, Munich, Germany), 50 μM ascorbic acid (Sigma-Aldrich, Munich, Germany), 10 ng $*$ mL^{-1} transforming growth factor beta (Sanver Tech, USA), 0.5 μg $*$ mL^{-1} insulin (Sigma-Aldrich, Munich, Germany), 0.5% antibiotics–antimycotics (Invitrogen, Karlsruhe, Germany), 1% FCS (Biowest, Nuaille, France)] or osteogenic [basic medium: alpha-MEM; 2 mM L-glutamine (Sigma-Aldrich, Munich, Germany), 60 μM ascorbic acid (Sigma-Aldrich, Munich, Germany), 10 mM β-glycerophosphate (Sigma-Aldrich, Munich, Germany), 0.1 μM dexamethasone (Sigma-Aldrich, Munich, Germany), 0.5% antibiotics–antimycotics (Invitrogen, Karlsruhe, Germany), 15% FCS (Biowest, Nuaille, France)] differentiation (Baumgartner et al., 2010; Steingen et al., 2008).

Adipogenic differentiation of hBMSCs was proven by Oil Red staining. Osteogenic differentiation of hBMSCs was proven by von Kossa staining. Chondrogenic differentiation was either proven by morphological Alcian blue (Okamoto et al., 2002) or Toluidine blue staining or by RT-PCT (see Section 2.3). Especially for the proof of maintenance of full differentiation capacities of hBMSCs after fESW treatment (see Section 2.4) we used morphological methods rather than RT-PCR to evaluate both the differentiation indicators described above and the morphology of hBMSCs. hBMSC morphology cannot be obtained by RT-PCR; however, the morphology represents a highly relevant marker in order to assess the influence of mechanical stimuli on the integrity of mechanically treated hBMSCs.

Proof of chondrogenic differentiation by RT-PCR

RNA of fESW-treated and -untreated hMSCs was extracted with the Peq-Gold TriFast reagent (PeqLab, Erlangen, Germany) according to the manufacturer's protocol. RNA was incubated with DNase (Invitrogen, Karlsruhe, Germany) for 15 min at room temperature to avoid DNA contamination. 1 μg RNA was used for RT-PCR. RNA was reverse-transcribed into cDNA using OmniScript reverse transcriptase kit (Qiagen, CA, USA) according to the manufacturer's protocol. For PCR, 1 μg of cDNA template was used, respectively. The following primers were used to prove for chondrogenic (collagen type II, GenBank number: NM_001844.4; forward: GAA CAT CAC CTA CCA CTG CAA G, reverse: GCA GAG TCC TAG AGT GAC TGA G) (Steingen et al., 2008), β-actin served as internal control, (GenBank number: NM_001101.3; forward: ACC TTC AAC ACC CCA GCC ATG TAC G, reverse: CTG ATC CAC ATC TGC TGG AAG GTG G). Resulting PCR products were analyzed using gel electrophoresis.

Application of focused and radial extracorporeal shock waves on hBMSCs

Cultured hBMSCs were subjected to focused (fESW) applications using the extracorporeal shock wave system Duolith®SD1 (Storz Medical AG, Trägerwilen, Switzerland) in 100 mm dishes (ibidi, Martinsried, Germany). fESW modes were applied to hBMSCs on a heat-stable foil and on an absorbing support surface (freshly prepared pork skin). In order to mimic the in vivo situation, culture dishes were filled completely with media and covered with freshly prepared pork skin (Fig. 1). For optimal coupling with the Duolith®SD1 system, an ultrasound gel (Parker Laboratories, Fairfield, NJ, USA) was placed on top of the pork skin. fESW applications were conducted as follows: continuous pulse, 1000 impulses, 4 Hz. Energy densities were as follows: 0 mJ $*$ mm^{-2} (control), 0.2 mJ $*$ mm^{-2}, and 0.3 mJ $*$ mm^{-2}. To evaluate the growth rate of hBMSCs before and after fESW applications, the cells were splitted after either control or after 0.2 mJ $*$ mm^{-2} application with 2000 cells $*$ cm^{-2}. After 24 h the cell number was again quantified. Every biological experiment was performed in quadruplicate and in a single session.

fESW treatments were also applied on cultured hBMSCs in order to test the influence of fESW on hBMSC differentiation potentials. Therefore, hBMSCs were treated with fESW as described above in this section and subsequently differentiated as described in Section 2.1.

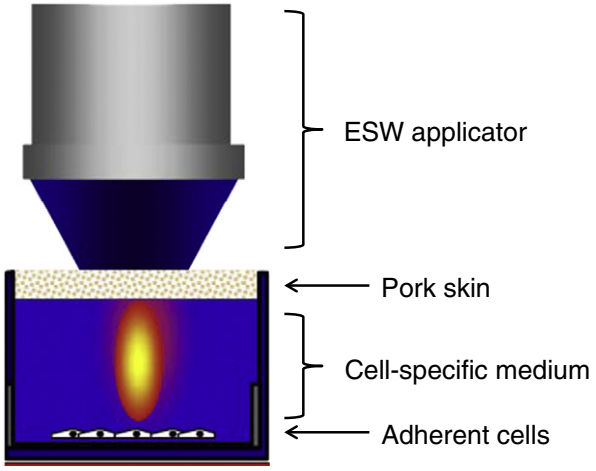

Figure 1 Cartoon of the experimental setup.

Immunocytochemistry

Prior immunocytochemistry, hBMSCs were fixed with 4% paraformaldehyde (PFA) for 1 h at room temperature before histological analysis (Steingen et al., 2008). hBMSC proliferation was detected by incubation with rabbit polyclonal anti Ki67 (Scholzen and Gerdes, 2000) antibody (dilution: 1:200, Abcam, Cambridge, UK) overnight at 4 °C. hBMSC apoptosis was detected by incubation with rabbit polyclonal anti caspase-3 (Patel et al., 1996) antibody (dilution: 1:500, BD, Heidelberg, Germany) overnight at 4 °C. Respective secondary antibodies (Dako Deutschland GmbH, Hamburg, Germany) were used with a dilution of 1:400. hBMSCs were examined with a Zeiss Axiovert 200 M light microscope coupled to a Axio Cam MR Video Camera (Carl Zeiss, Jena, Germany). Digitally captured images (200× magnification) were analyzed by assessment of optical densitometry with the software ImageJ® (National Institutes of Health, USA). Negative control hBMSCs were processed as were experimental hMSCs; however, primary antibody incubations were substituted by incubation with 0.8% TBS.

Analysis of the cytoskeletal morphology

To visualize directed F-actin stress fibers and disorganized actin fibers of the cytoskeleton, fESW-treated and -untreated hBMSCs were washed in 0.05 M TBS followed by permeabilization with 0.25% Triton X-100, washed again with TBS and subsequently dyed with phalloidin/Alexa Fluor488 (dilution 1:40 in TBS, Molecular Probes, Invitrogen, Leiden, Netherland) for 20 min (Pellegrin and Mellor, 2007; Spallarossa et al., 2010) and covered with 4,6-diamidino-2-phenyl-indol (DAPI) containing mounting medium (Vectashield, Vector Laboratories). For analysis of directed F-actin stress fibers and disorganized actin fibers, the total number of DAPI-positive hBMSCs was quantified using a fluorescence microscope (Axiovert 200 M, Carl Zeiss, Jena, Germany). Directed F-actin stress fibers as well as disorganized actin fibers were related to the total number of DAPI-positive hMSCs. Additionally, the percentage of disorganized actin fibers of hBMSCs was documented in fESW-treated -untreated hBMSCs, indicating structural rearrangements of the cytoskeleton (Jaalouk and Lammerding, 2009; Spallarossa et al., 2010) in response to fESW applications.

Boyden chamber assay

The migration assay was performed in a modified Boyden chamber assay as described previously (Schmidt et al., 2006). In brief, after hBMSCs were grown to a confluent monolayer and the dishes were treated with singular applications of fESW. Untreated dishes served as controls. After fESW treatments, hBMSCs were detached by Accutase and counted. $5 * 10^4$ cells were seeded on top of the specific migration filter (8 μm pores, Falcon® HTS Fluoro Blok™, Becton Dickinson Labware Europe, Le Pont De Claix, France) and were incubated for 8 h at 37 °C, 5% CO_2, and 95% humidity in 20% FCS-containing alpha-MEM in a 24-well plate (Tissue Culture Plate, Becton Dickinson Labware Europe, Le Pont De Claix, France). Subsequently, hBMSCs were fixed using 4% paraformaldehyde (PFA). The cells were covered using mounting medium containing DAPI (Vectashield, Vector Laboratories). The number of migrated hBMSCs was counted and documented using a fluorescent microscope (Axiovert 200 M, Carl Zeiss Microscopy, Jena, Germany). Only completely migrated cells were taken into account for further analysis.

Wound healing and scratch assay of hMSCs

In vitro wound healing assays (scratch assays) were performed as described previously (Faber-Elman et al., 1996). After fESW application, the treated hBMSCs were incubated for 24 h in the Axiovert 200 M light microscope (Carl Zeiss, Jena, Germany) under cell culture conditions (37 °C, 5% CO_2, and 95% humidity) in 20% FCS-containing alpha-MEM. Time lapse video analysis was used to document the wound healing process; every 10 min pictures were taken with a 5× objective (A-Plan 5×/0.12, Carl Zeiss, Jena, Germany). The wound area was calculated with the Axiovision software (Carl Zeiss, Jena, Germany).

Cell tracking assay of hMSCs

To monitor cell movements, cell tracking analysis of hBMSCs in response to fESW applications was performed as described (Schmidt et al., 2006). In brief, hBMSCs were plated at a density of 2000 cells $*$ cm^{-2} on cell culture dishes (Ibidi, Martinsried, Germany). ESW-treated and untreated control hBMSCs were monitored by time lapse video for 24 h until hBMSCs reached a confluence of about 40%. During that time, the cells were incubated for 24 h in the Axiovert 200 M light microscope (Carl Zeiss, Jena, Germany) under cell culture conditions (37 °C, 5% CO_2, and 95% humidity) in 20% FCS-containing alpha-MEM. Every 10 min, pictures were taken with a 5× objective (A-Plan 5×/0.12, Carl Zeiss, Jena, Germany); data were exported to Metamorph microscopy analysis software (Molecular Devices, Sunnyvale, CA, USA) for further analysis. The analyzed parameter included the velocity of hBMSCs, their distance [pixel] per 10 min and their total distance to the starting point after 24 h.

Statistics

One-way analysis of variances (ANOVA) of each fESW condition was performed using Statistica software package (Statistica for Windows 7.0, Tulsa, USA). If the one-way ANOVA was significant, individual differences between tested conditions were tested by applying a post hoc test (Duncan's multiple comparison test). Statistical significance was considered for $p < 0.05$. A paired Student's *t*-test was applied to test the applied stimulus of 0.2 mJ * mm^{-2} compared to control condition on hBMSC growth rate and wound healing/scratch assay. Statistical significance was considered for $p < 0.05$. Data are presented as mean ± standard error of means (S.E.M.).

Results

The present study examined dose-dependent modifications of fESW-generated mechanical stimuli on cellular behaviors of hBMSCs. The focus of the present study was on the cell biological effects, such as proliferation, apoptosis, growth rate, actin cytoskeletal rearrangements and cell migration properties of fESW treatments. Additionally, we studied the differentiation potential of fESW-treated hBMSCs compared to untreated hBMSCs.

Characterization of hBMSCs

As hBMSCs are a rare population within the human bone marrow, we sought to rigorously enrich cell preparations for true hBMSCs in terms of representative surface markers using FACS (Baumgartner et al., 2010; Pittenger et al., 1999; Steingen et al., 2008). Subsequently, the identity of hBMSC preparations was confirmed by different means. fESW-untreated hBMSCs were characterized by adipogenic, chondrogenic and osteogenic differentiation assays (Figs. 2A,B). Fig. 2A shows fESW-untreated hBMSC morphology at different confluence levels (Figs. 2A1, A2) as well as adipogenic (Fig. 2A3, control Fig. 2A4), osteogenic (Fig. 2A5, control Fig. 2A6), and chondrogenic (Fig. 2A7, control Fig. 2A8) differentiation assays. Additionally, the chondrogenic differentiation capacity of fESW-untreated hBMSCs was confirmed by RT-PCR (Fig. 2B).

As the growth rate depends on cell proliferation and apoptosis (Klotz et al., 2012), we next aimed to quantify the effects of different fESW applications on these cellular processes by investigating markers of proliferation and activated apoptosis in hBMSCs in more detail.

Proliferation and apoptosis of hBMSCs in response to fESW applications of different intensities

To determine the effects of fESW application on hBMSC proliferation and apoptosis, hBMSCs were immunohistochemically stained for Ki67 and caspase-3, respectively. Ki67 represents a common proliferation marker and is expressed in all active phases of the cell cycle, except the G0 phase (Heidebrecht et al., 1996; Traut et al., 1998). hBMSCs were stained 6 h and 12 h after fESW applications. Compared to the control conditions, application of fESW (0.2 mJ * mm^{-2}) resulted in a significant increase in proliferative hBMSCs after both 6 h ($p < 0.01$) and 12 h ($p < 0.05$) (Fig. 3A). Application of 0.3 mJ * mm^{-2} showed no effects after 6 h ($p > 0.05$), but a significant decrease of proliferative hBMSCs after 12 h ($p < 0.01$) (Fig. 3A) compared to control hBMSCs.

Activation of apoptosis of hBMSCs after fESW treatments was investigated using the marker caspase-3 (Patel et al., 1996). hBMSCs were stained 6 h and 12 h after fESW applications. Compared to control conditions, the application of fESW (0.2 mJ * mm^{-2}) resulted in a significant increase in apoptotically activated hBMSCs after 6 h ($p < 0.05$) (Fig. 3B). However, this effect was transient as after 12 h, the number of caspase-3 positive cells decreased even below control levels, although this difference was not significant (Fig. 3B). Application of 0.3 mJ * mm^{-2} resulted in a significant increase in apoptotically activated hBMSCs after both 6 h ($p < 0.01$) and 12 h ($p < 0.01$) (Fig. 3B). In summary, these results show that proliferation and apoptosis are influenced by fESW-induced mechanical stimulation in hBMSCs. Importantly, both parameters can significantly be influenced by fESW applications in a dose-dependent manner. Of all conditions tested, the fESW with an intensity of 0.2 mJ * mm^{-2} was found to be an optimal stimulation, combining maximal induction of proliferation with minimal activation of apoptosis.

Determination of growth rate of hBMSCs in response to fESW applications

hBMSC growth rates of were determined in order to qualitatively characterize hBMSCs in culture (Arnhold et al., 2006) as well as to examine the effects of fESW (0.2 mJ * mm^{-2} applications). The growth rate ($W = dN * dt^{-1}$) describes the reproduction of hBMSCs per time unit, in our case within 24 h. The proliferation potential of control samples strongly suggests that the start material contained highly enriched hBMSCs. As the fESW (0.2 mJ * mm^{-2}) led to the highest increase of hBMSC proliferation and even reduced activation of apoptosis, we focused on this stimulation. fESW applications were observed to significantly ($p < 0.01$) stimulate hBMSC reproduction (around $1.25 * 10^5$ cells * $24\ h^{-1}$, Fig. 3C), which support our findings of increased proliferation and decreased apoptotically activated hBMSCs. These results indicate important regulatory influences of fESW-induced mechanical stimulations on growth rates of hBMSCs and the increased cell number is in line with other studies (Higuera et al., 2009). To further determine cell biological characteristics of untreated compared to fESW-treated hBMSCs, we next aimed to quantify the effects of shock wave-induced mechanical stimuli on migration properties of hBMSCs in more detail.

Boyden chamber assay

The migratory behavior of hBMSCs is known to be critical for their successful application in tissue regeneration (Li and Jiang, 2011). Migratory properties of hBMSCs after fESW applications were assessed by the use of a modified Boyden chamber assay (Schmidt et al., 2006). Migrated hBMSCs were assessed in a meander-shaped manner to avoid duplicate determinations.

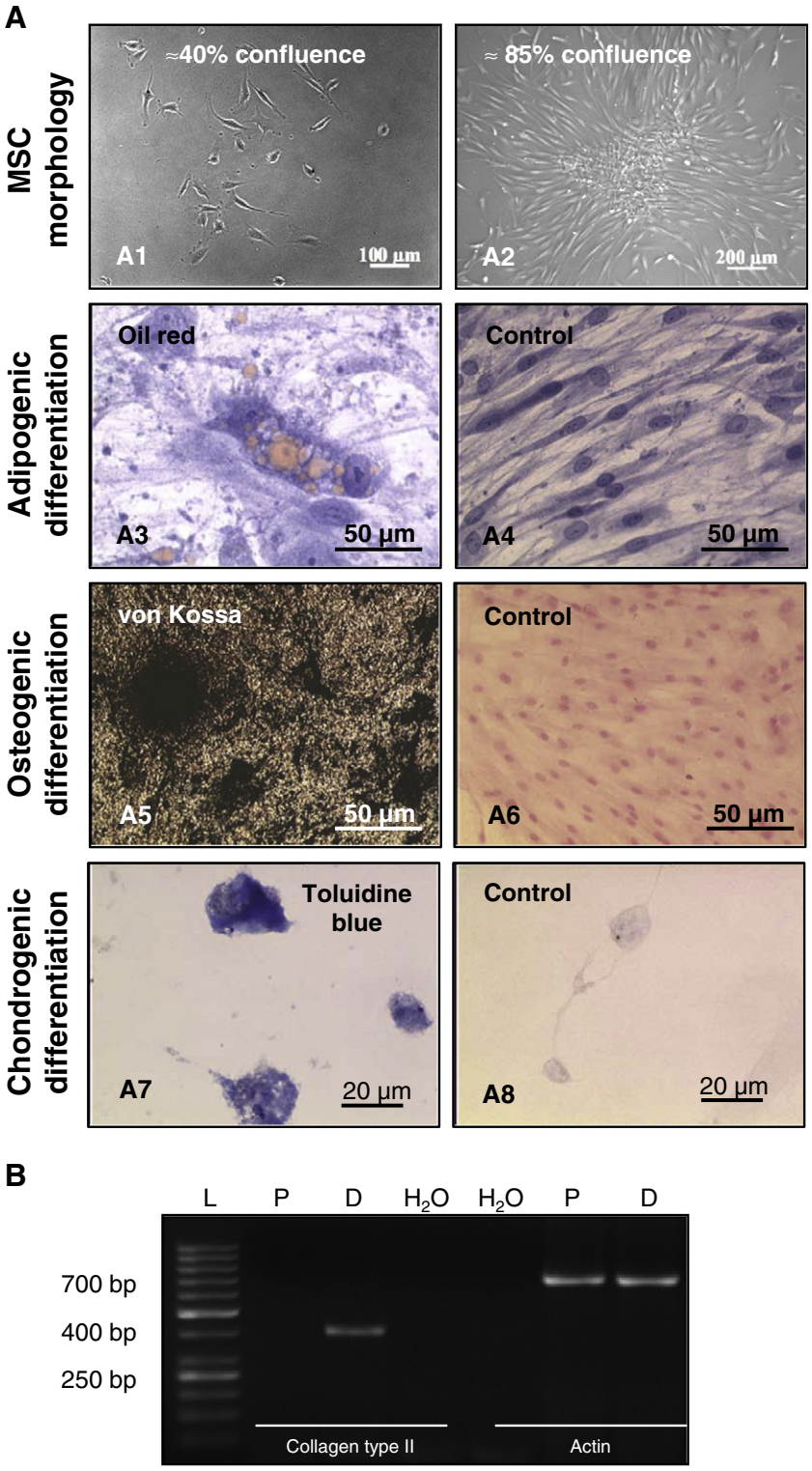

Figure 2 hBMSC characterization. (A) Morphological and biochemical approaches for characterizing hBMSCs. (A1, A2) Undifferentiated hBMSCs grown in monolayer culture shown at different confluence levels. A1 shows hBMSCs at a confluence of about 40%; A2 shows hBMSCs at a confluence of about 85%. (A3, A4) Adipogenic differentiation of hMSCs. A3 depicts Red Oil staining of lipid vacuoles after three weeks of adipogenic stimulation; A4 shows control hBMSCs stained with hematoxylin/eosin. (A5, A6) Osteogenic differentiation of hBMSCs. A5 shows von Kossa staining of calcium deposits after three weeks of osteogenic stimulation; A6 shows control hBMSCs stained with nuclear fast red-aluminum sulfate solution. (A7, A8) Chondrogenic differentiation of hBMSCs. A7 shows Toluidine blue staining after three weeks of chondrogenic stimulation; A8 shows control hBMSCs. (B) Chondrogenic differentiation (D) of hBMSCs proven by RT-PCR, but not in the proliferation approach (P). H_2O was used as a negative control. Actin served as an internal housekeeping gene and showed no regulation by either D or P approaches. No signal was observed in the H_2O control.

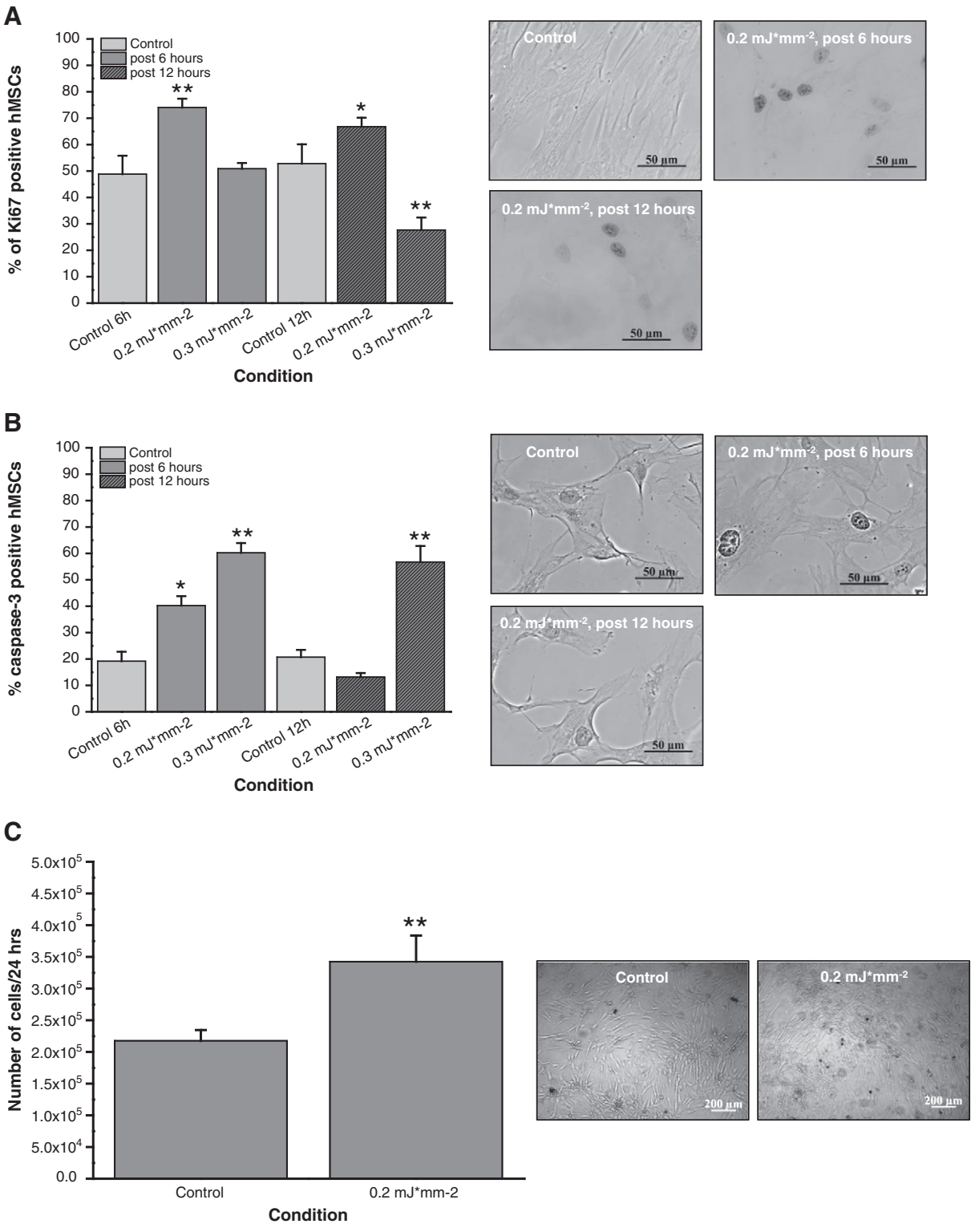

Figure 3 hBMSC proliferation, apoptosis, and growth rate. (A) The diagram shows proliferative Ki67 positive hBMSCs in response to fESW treatment. Compared to control hBMSCs, fESW treatments increased the percentage of Ki67 positive hBMSCs 6 and 12 h post-treatment, with the exception of the 0.3 mJ $*$ mm^{-2} treatment after 12 h. The pictures in the right panel reflect Ki67 stained hBMSCs 6 and 12 h post 0.2 mJ $*$ mm^{-2} treatment compared to untreated control hBMSCs. (B) The diagram shows apoptotic, caspase-3 positive hBMSCs in response to fESW treatment. Compared to control hBMSCs, fESW treatments partially induced increased percentages of caspase-3 positive hBMSCs 6 and 12 h post-treatment. Importantly, 0.2 mJ $*$ mm^{-2} resulted in a decreased percentage of caspase-3 positive hBMSCs compared to control hBMSCs 12 h post-treatment. The pictures in the right panel show caspase-3 stained hBMSCs 6 and 12 h post 0.2 mJ $*$ mm^{-2} treatments compared to untreated control hBMSCs. (C) The growth rate was significantly increased after fESW (0.2 mJ $*$ mm^{-2}) compared to untreated hBMSCs within 24 h. The pictures in the right panel show monolayer under both control and fESW (0.2 mJ $*$ mm^{-2}) conditions. *$p < 0.05$, **$p < 0.01$.

fESW applications (0.2 mJ * mm^{-2}) resulted in significantly increased numbers ($p < 0.05$, Fig. 4A) of completely migrated hBMSCs, whereas application of 0.3 mJ * mm^{-2} inhibited the migration of hBMSCs significantly ($p < 0.05$, Fig. 4A). These results demonstrate the existence of a physiological threshold above which mechanical stimulations seem to be counterproductive for the induction of hBMSC migration. Therefore, fESW-induced mechanical stimulations induce dose-dependent biological effects on hBMSCs.

Actin cytoskeleton arrangement of hBMSCs

In hBMSCs F-actin is well-organized in linear stress fibers (Fig. 4B). Cytoskeletal architecture, such as directed F-actin stress fibers, is known to be crucial for cell migration (Pellegrin and Mellor, 2007). Therefore, it was tested whether mechanical stimuli can modify the actin cytoskeleton. Fluorescence-labeled phalloidin (Alexa Fluor488) was used to visualize the F-actin cytoskeleton of hBMSCs (Pellegrin and Mellor, 2007; Spallarossa et al., 2010). hBMSC cytoskeletal organization was determined 0 min and 30 min after fESW applications.

fESW (0.2 mJ * mm^{-2} and 0.3 mJ * mm^{-2}) treatments resulted in an initially significantly ($p < 0.05$) decreased portions of directed F-actin fibers. However, 30 min after 0.2 mJ * mm^{-2} application the cells recovered and presented with a massive assembly of directed F-actin fibers ($p < 0.05$) (Fig. 4B), while the cells were only able to reassemble very few fibers within 30 min post 0.3 mJ * mm^{-2} treatment (Fig. 4B).

These results suggest that the stimulation with fESW (0.2 mJ * mm^{-2}) might prove optimal to induce migration of hBMSCs. We tested this assumption directly using different assays.

Disorganized and partly destroyed actin fibers indicate rearrangements of the cellular cytoskeleton (Morita et al., 1994; Spallarossa et al., 2010). Therefore, the portion of disorganized actin fibers was also quantified in response to fESW applications 0 min and 30 min after treatment. Compared to the control condition, fESW treatment (0.2 mJ * mm^{-2} and 0.3 mJ * mm^{-2}) resulted in a significantly ($p < 0.05$ for each) increased portion of disorganized actin fibers in hBMSCs at 0 min post-treatment (Fig. 4C). A similar picture was observed at 30 min ($p < 0.05$), but only after 0.3 mJ * mm^{-2} fESW application (Fig. 4C). In contrast, but in line with the directed F-actin fibers (Fig. 4B), 0.2 mJ * mm^{-2} significantly ($p < 0.01$) reduced disorganized actin fibers at 30 min post-treatment (Fig. 4C). These results indicate important divergent influences of fESW application in a dose-dependent manner and indicate 0.2 mJ * mm^{-2} as most beneficial for directed F-actin assembly.

Cell tracking assay

To assess hBMSC movements, cell-tracking assays were performed. fESW-treated and -untreated hBMSCs were photographed every 10 min over a time course of 24 h to document hBMSC movement in response to fESW applications. The treatment of hBMSCs with any fESW condition resulted in comparable significant increases in movement velocities of hBMSCs compared to control hBMSCs ($p < 0.05$, Fig. 5, see also video data 1 and 2 in the supplementary data). These results lead to the assumption that mechanical stimulations exerted by fESW of divergent intensities positively influence migration and distance velocities of hBMSCs. This observation might be of great impact for medical therapies as hBMSCs often show low infiltrations into diseased tissues (Hofmann et al., 2005).

Wound healing assay

Due to the results obtained from the Boyden chamber assays, which indicated a positive influence of fESW (0.2 mJ * mm^{-2}) applications on hBMSC migration, wound-healing assays were conducted with hBMSCs using the same treatment. These assays test whether the increased cell movements are directed or whether the mechanical stimulation causes random movements leaving the cells incapable of directed migration. In this system only directed migration results in a more efficient wound closure. In comparison to the control conditions, fESW application of 0.2 mJ * mm^{-2} resulted in an increased portion of wound closure at both 4 h ($p < 0.05$) and 8 h ($p < 0.01$) post fESW treatment (Fig. 5B, see also video data 3 and 4 in the supplementary data). Consequently, the time required to complete wound closure was significantly decreased ($p < 0.05$, Fig. 5C). These observations clearly illustrate that ESW-induced mechanical stimulations have a positive influence on the movement and velocity of directed hBMSC migration, demonstrating the potential of mechanical stimulations for clinical hMSC applications.

hBMSC differentiation potential into adipocytes, chondrocytes, and osteocytes after fESW treatment

After investigating cell biological behaviors of hBMSCs in response to fESW treatment we sought to study whether the differentiation potential of mechanically treated hBMSCs were still viable and whether the differentiation potential correlated in a certain manner to the cell biological results we obtained from our assays. Therefore, hBMSCs were subjected to both 0.2 mJ * mm^{-2} and 0.3 mJ * mm^{-2} fESW treatments and differentiated into adipogenic, chondrogenic, and osetogenic cells, whereas fESW-treated hBMSCs were compared to mechanically untreated hBMSCs (Fig. 6). As shown in Fig. 6, both fESW treatments directed hBMSCs into the three lineages as also observed under control conditions. This is of paramount interest, because mechanically treated hBMSCs do not lose their differentiation potentials, but remain able to differentiate into adipocytes, chondrocytes, and osteocytes. While the adipogenic differentiation was unaffected by fESW treatments (Figs. 6A–C), we observed some minor, but notable differences between the fESW treatment conditions during osteogenic and chondrogenic differentiations. Compared to control (Fig. 6D) and 0.2 mJ * mm^{-2} (Fig. 6E), the osteogenic differentiation potential was slightly reduced after 0.3 mJ * mm^{-2} application (Fig. 6F, dashed arrows). Furthermore, compared to control (Fig. 6 G, arrows) and 0.3 mJ * mm^{-2} (Fig. 6I, arrows) conditions we observed an altered chondrogenic differentiation potential after 0.2 mJ * mm^{-2} treatment (Fig. 6 H, arrow heads). In the 0.2 mJ * mm^{-2} condition the chondrogenic cells seem to be more organized and aligned compared to the control and

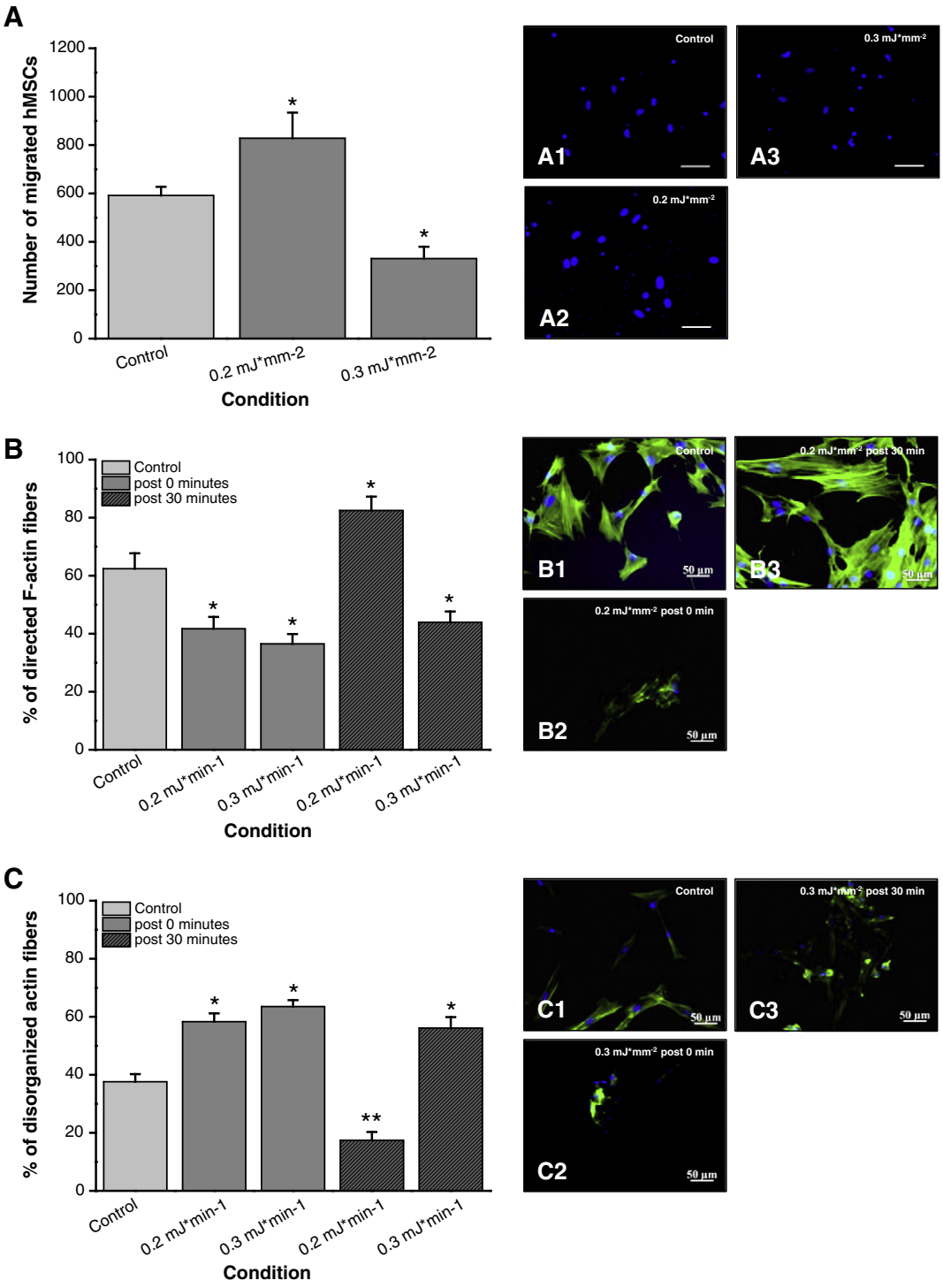

Figure 4 hBMSC migration, directed F-actin, and disorganized F-actin. (A) hBMSC migration behavior was observed by Boyden chamber assays. The diagram shows that only the fESW (0.2 mJ * mm^{-2}) treatment resulted in an increased number of migrated hBMSCs. The pictures in the right panel show DAPI positive hBMSCs transmigrated through the 8 μm pore. Control and fESW treatments (0.2 mJ * mm^{-2} and 0.3 mJ * mm^{-2}) are shown. (B) The diagram shows directed F-actin fibers in response to fESW treatment. As depicted, only the 0.2 mJ * mm^{-2} treatment resulted in an increased percentage of directed F-actin fibers in hBMSCs compared to control hBMSCs. The pictures in the right panel show directed F-actin fibers in control hBMSCs as well as fESW-treated (0.2 mJ * mm^{-2}) hBMSCs 0 and 30 min post-treatment. (C) The diagram shows disorganized actin fibers in response to fESW treatment. As depicted, fESW treatments increased the percentage of disorganized actin fibers at 0 min post-treatment. However, at 30 min post-treatment, 0.2 mJ * mm^{-2} applications resulted to significantly reduced percentage of disorganized actin fibers, whereas 0.3 mJ * mm^{-2} significantly increased disorganized actin fibers compared to control condition. The pictures in the right panel show disorganized actin fibers in control as well as fESW-treated (0.2 mJ * mm^{-2}) at 0 and 30 min post-treatment. *$p < 0.05$, **$p < 0.01$.

0.3 mJ * mm^{-2} conditions, indicating a more effective chondrogenic differentiation after 0.2 mJ * mm^{-2} application compared to controls and 0.3 mJ * mm^{-2}. Similarly, we observed this phenomenon also by means of the second chondrogenic evidence, Toluidine blue (Fig. 6 K, arrow heads) when compared to control (Fig. 6J) and 0.3 mJ * mm^{-2} (Fig. 6 L). These data indicate that hBMSCs maintain their full differentiation potentials even after fESW treatments, while minor, but relevant differences can be observed proving that 0.2 mJ * mm^{-2} energy density seems to be the most beneficial application. These data confirm that 0.2 mJ * mm^{-2} might prove optimal for hBMSCs preconditioning, as suggested by the data shown above.

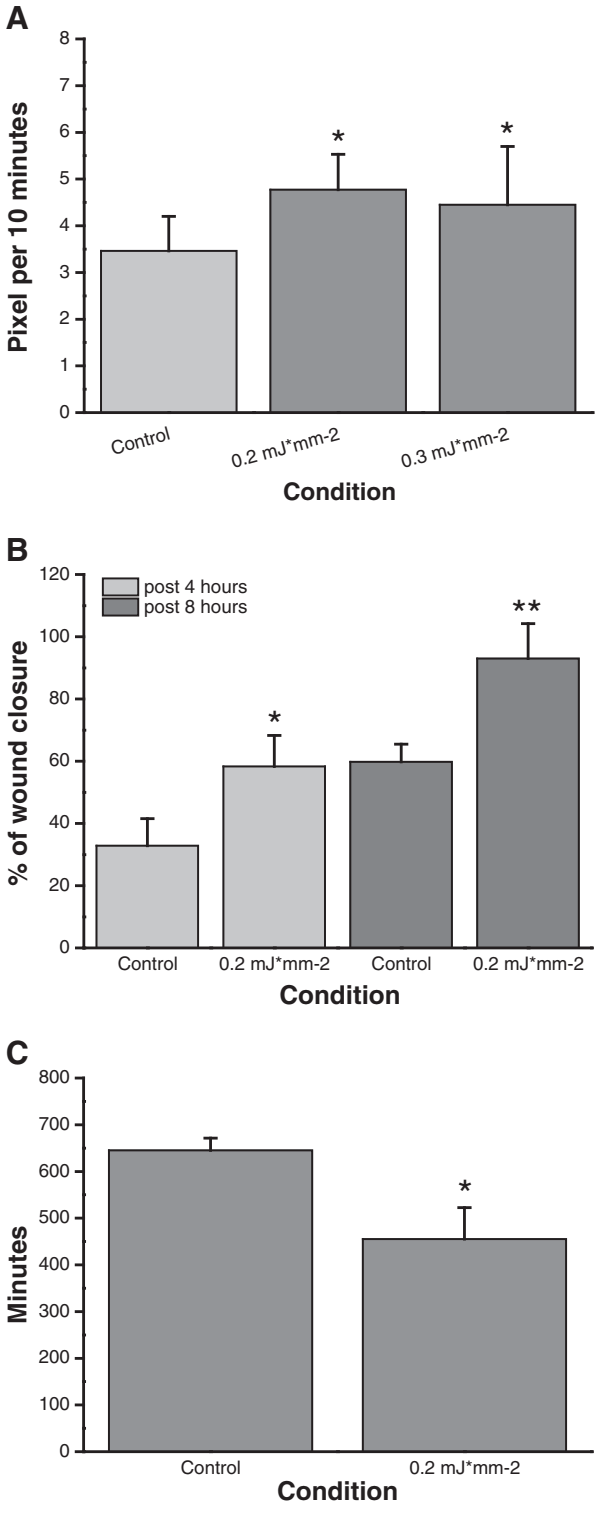

Discussion

While the potential usefulness of hBMSCs in regenerative medicine is undisputed, the efficacy of hBMSC-based treatments appears to decisively depend upon how effectively transplanted hBMSCs can be targeted persistently to the diseased area and how functional these cells are in terms of the regeneration process. We hypothesized in the present study that fESW modify cell biological behavior of hBMSCs and further, that this allows for mechanical priming of hBMSCs in order to improve their biological properties important for tissue regeneration (Ingber, 2006). fESW have been shown to be a source of mechanical impacts and have been used successfully in regenerative cardiac medicine (Nishida et al., 2004). Additionally, a recent study proposed positive effects of ESW applications in bone marrow-derived endothelial progenitors to improve ischemic areas in rodent critical limb ischemia (Yeh et al., 2012), demonstrating the significance of ESW also in other tissues. However, in these studies the mechanistic basis or possible cellular players were not explored.

In hBMSC-based cell therapy, the number of cells present in the target tissue can be increased either by upscaling the total amount of transplanted cells or by repeated delivery. A myriad of studies has used different approaches, including genetic manipulation, to control the behavior of hBMSCs; however, thus far, no approach has proved to be therapeutically feasible. We hypothesized that fESW applications would stimulate hBMSC expansion without the need for genetic manipulation, making this approach directly compatible with clinical use.

To quantify the proliferative stimulation of fESW applications in hBMSCs, the proliferation marker Ki67 (Heidebrecht et al., 1996; Traut et al., 1998) was used. We observed that fESW application results in proliferation rates about 75% greater than those of untreated cells, which is much higher than the 20–60% increase described in previous mechanical stimulation studies (Arnhold et al., 2006; Schmidt et al., 2006). Additionally, we found the proliferative effect to last nearly 12 h post

Figure 5 Cell tracking assay and wound healing/scratch assay. (A) The diagram shows that applications of different fESW treatments result in significantly increased migration velocities of fESW-treated hBMSCs compared to untreated control. See also video data 1 and 2 (supplementary data). (B) The diagram shows the percentage of wound closure by fESW-treated (0.2 mJ * mm^{-2}) hBMSCs 4 and 8 h post-treatments. fESW treatment of hBMSCs results in significantly increased percentage of wound closure at both investigated time points compared to the respective control situations. See also video data 3 and 4 (supplementary data). (C) The diagram shows that the time needed for a complete wound closure was significantly reduced after fESW (0.2 mJ * mm^{-2}) treatment compared to untreated control hBMSCs. *$p < 0.05$, **$p < 0.01$.

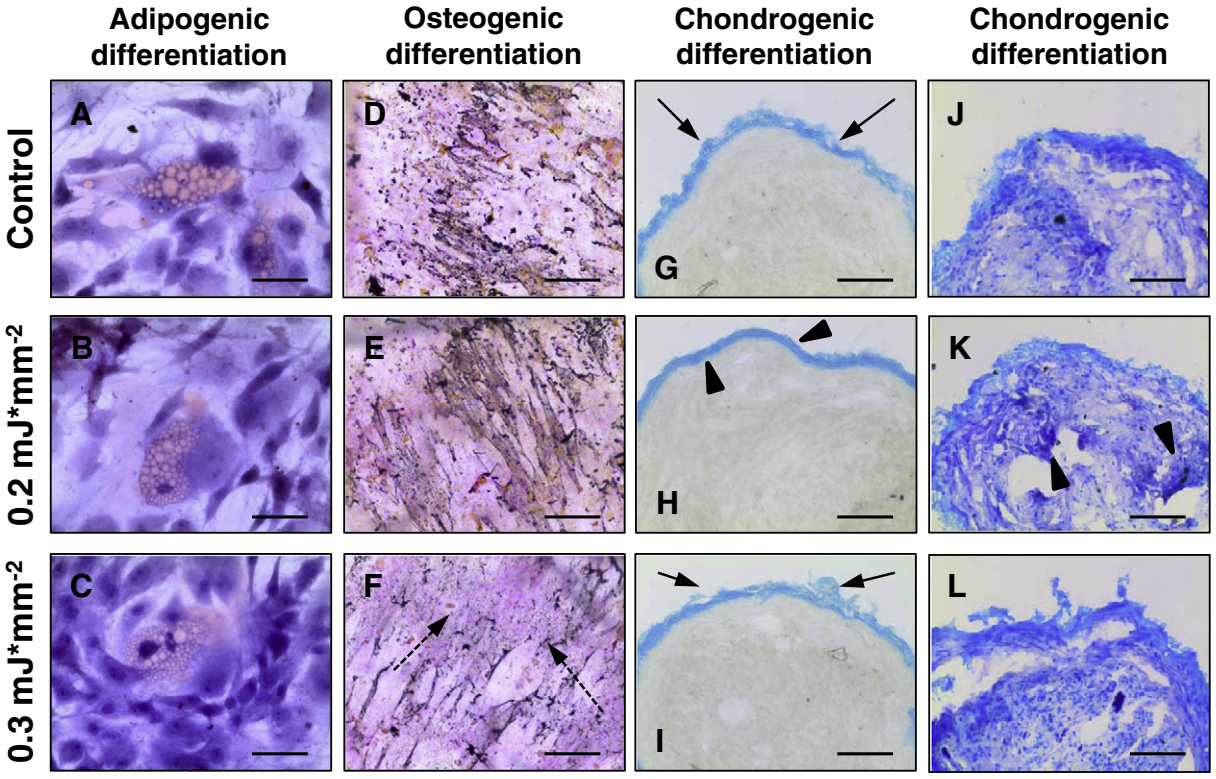

Figure 6 Maintenance of hBMSC differentiation capacities after fESW treatment. hBMSCs were either treated with fESW (0.2 mJ * mm^{-2}/0.3 mJ * mm^{-2}) or remained untreated (control). The differentiation capacities were proven by Red Oil staining (adipogenic cells, A–C), von Kossa staining (osteogenic cells, D–F), Alcian blue (chondrogenic cells, G–I) or by Toluidine blue staining (chondrogenic cells, J–L). As demonstrated, hBMSCs maintain their full differentiation capacities after both fESW treatments compared to control conditions. However, some minor, but notable differences between the fESW treatment conditions during osteogenic and chondrogenic differentiation were observed. Compared to control (D) and 0.2 mJ * mm^{-2} (E), the osteogenic differentiation potential was slightly reduced after 0.3 mJ * mm^{-2} application (F, dashed arrows). Furthermore, compared to control (G, arrows) and 0.3 mJ * mm^{-2} (I, arrows) conditions we observed an altered chondrogenic differentiation potential after 0.2 mJ * mm^{-2} treatment (H, arrow heads). In the 0.2 mJ * mm^{-2} condition the chondrogenic cells seem to be more organized and aligned compared to the control and 0.3 mJ * mm^{-2} conditions, indicating a more effective chondrogenic differentiation after 0.2 mJ * mm^{-2} application compared to controls and 0.3 mJ * mm^{-2}. Similarly, we observed this phenomenon also by means of the second chondrogenic evidence, Toluidine blue (k, arrow heads) when compared to control (J) and 0.3 mJ * mm^{-2} (L). Bar in A–C: 50 μm; bar in D–F: 25 μm; bar in G–L: 10 μm.

fESW treatment, exceeding the effects of mechanical stimulations previously described.

It has been demonstrated that mechanical impacts can induce apoptosis in various cells including cancer cells (Kato et al., 2000; Kearney et al., 2008). In the present study, we found that this observation holds true for hBMSCs; however, the intensity of the mechanical stimulation appears to be of central importance. After an initial increase, the apoptosis rate of cells 12 h after application with 0.2 mJ * mm^{-2} fESW was significantly reduced compared to control levels. Combined, these data demonstrate that fESW-induced mechanical stimulations result in increased hBMSC growth rates. As it was demonstrated recently that different culture media exert different effects of hBMSC growth rates (Ben et al., 2012), we speculate that improved culture conditions, combined with the right choice of mechanical stimulations, will provide the best outcomes for hBMSC expansion.

Directed stress fibers were shown to increase cell migration (Kreis and Birchmeier, 1980; Spallarossa et al., 2010) and determine the migration direction (Rid et al., 2005). Our experiments demonstrate that the fESW-induced mechanical stimulations result in significant increases in hBMSC F-actin stress fiber formation and migration, indicating a positive cell biological effect of the applied stimuli on these cells in a dose-dependent manner. More precisely, fESW applications resulted in a significant reduction of directed F-actin fibers, with the exception of 0.2 mJ * mm^{-2} at 30 min post-treatment. Therefore, the formation of F-actin stress fibers in hBMSCs strongly depends on the applied stress dose.

Disorganized actin fibers can limit cell migration (Spallarossa et al., 2010). The formation of disorganized actin fibers indicates a rearrangement of the cytoskeleton and, therefore, can be independent of directed F-actin stress fibers (Jaalouk and Lammerding, 2009). As demonstrated, fESW applications resulted in increased disorganized actin fibers after treatment along with a massively increased portion of directed F-actin fibers concurring with a low formation of disorganized actin fibers post-intervention. Both events might contribute synergistically to the improved migratory

properties of preconditioned hBMSCs. In summary, our results show that applications of mechanical impacts induced by fESW might particularly improve BMSC migration.

As it was reported previously that mechanical stimuli cannot increase the migration of hBMSCs (Ode et al., 2011) we tested this in detail using three different assay systems. All of our experiments clearly showed that application of fESW results in increased hBMSC migration. However, the results of these respective studies are difficult to compare as the source of mechanical stimulation differed and the differently applied energy densities could possibly explain the discrepancies. Particularly, our data show that the nature and intensity of mechanical stimulation are of key importance for the cellular response. Future investigations should carefully address the migration behavior of hBMSCs in response to defined mechanical treatments; we have strong evidence that this kind of hBMSC preconditioning is a particularly promising approach to improve hBMSC-based therapies. In this context, also less specified cells, such as fibroblasts or muscle cells, should be investigated, because it is reasonable that these cells might also react in a comparable manner, as they are also mechano-sensitive.

Additionally, Schmidt et al. (2006) demonstrated a positive influence of bFGF on the wound healing ability of hBMSCs. Therefore, we propose that a combined treatment with both growth factors and mechanical stimulations could further improve the tissue regenerative capacities of hBMSCs. Alternatively, it would be interesting to test whether mechanical stimulation leads to secretion of bFGF and/or other growth or trophic factors that could act in an autocrine fashion and might be mechanistically responsible for the effects observed here.

It is interesting that the stimulation with fESW ($0.2\ mJ * mm^{-2}$) had optimal effects on BMSCs' biological parameters in our experimental setup. The fact that mechanical shockwaves fESW have been beneficial to the healing process in in vivo experiments in combination with our data suggests that BMSCs are actively involved in the biological processes leading to functional improvements. As this has previously been assumed but not demonstrated (Nishida et al., 2004), our data provide the rationale for the in vivo use of mechanical stimulation for hBMSC-based treatments.

This rational is further strengthened by our finding that the differentiation potentials of hBMSCs remains fully preserved after fESW treatments compared to untreated control conditions. These paramount data also explain finding from the literature that ESW treatment beneficially induces de novo bone formation in vivo (van der Jagt et al., 2011; van der Jagt et al., 2013). However, the energy density seems to be the limiting factor. As discussed above, we suggest that $0.2\ mJ * mm^{-2}$ is the most beneficial stimulus in our setup for priming of hBMSCs. This hypothesis is also supported by the finding that hBMSCs show best differentiation characteristics following treatment with $0.2\ mJ * mm^{-2}$ when compared to control and $0.3\ mJ * mm^{-2}$ conditions.

It will be interesting for future studies to investigate effects of fESW, but also radial ESW as another ESW source, on other cell types, e.g. cardiomyocytes or skeletal muscle precursors in order to evaluate ESW effects on these important adult cell types. However, the optimal energy density is likely to differ between different experimental setups and of course between patients in medical therapy applications, why special caution has to be put on this issue in future studies. Together, due to optimal effects of the same stimulation for multiple aspects of hBMSC behavior and the unproblematic use of this technique in a clinical setting, fESW-mediated preconditioning of hBMSCs presents an elegant tool in regenerative medicine.

5. Conclusion

The presented data describe fESW as a potential approach to manipulate hBMSC behavior for clinical applications. This approach appears particularly promising as it suggests that mechanical stress preconditions hBMSCs for improved therapeutic performance without any genetic manipulation or loss of differentiation potential. Because of the high potential of the present findings to benefit the healing process of adult degenerative tissue, it is currently tested whether they can be validated in vivo.

Additionally, our study defines a working intensity and nature of fESW-derived mechanical stimuli resulting in improved BMSC behavior, whereby the optimal intensity and application time will differ dependent of the experimental setup, the patient, and importantly, the used ESW device. This report identifies how hBMSCs change proliferation, migration, survival and, in combination with the work of others, also paracrine activity (Gnecchi et al., 2005) and proteolytic activity in response to mechanical stress (Kasper et al., 2007).

Acknowledgments

The authors thank Kathryn D. Rodgers for critically reading the manuscript. The authors also thank Anika Voss, Department of Molecular and Cellular Sport Medicine, German Sport University Cologne, Germany, for technical assistance. The study was funded by a grant from STORZ Medical AG, Tägerwilen, Switzerland. This manuscript is dedicated to memories of Helmut Neuland (†) for his tireless effort to realize this project.

Appendix A. Supplementary data

Supplementary data to this article can be found online at http://dx.doi.org/10.1016/j.scr.2013.05.010.

References

Arnhold, S., Klein, H., Klinz, F.J., Absenger, Y., Schmidt, A., Schinkothe, T., Brixius, K., Kozlowski, J., Desai, B., Bloch, W., et al., 2006. Human bone marrow stroma cells display certain neural characteristics and integrate in the subventricular compartment after injection into the liquor system. Eur. J. Cell Biol. 85, 551–565.

Baumgartner, L., Arnhold, S., Brixius, K., Addicks, K., Bloch, W., 2010. Human mesenchymal stem cells: influence of oxygen pressure on proliferation and chondrogenic differentiation in fibrin glue in vitro. J. Biomed. Mater. Res. A 93, 930–940.

Ben, A.N., Jenhani, F., Regaya, Z., Berrais, L., Ben, O.T., Ducroq, E., Domenech, J., 2012. Phenotypical and functional characteristics of mesenchymal stem cells from bone marrow: comparison

of culture using different media supplemented with human platelet lysate or fetal bovine serum. Stem. Cell Res. Ther. 3, 6.
Chang, K.V., Chen, S.Y., Chen, W.S., Tu, Y.K., Chien, K.L., 2012. Comparative effectiveness of focused shock wave therapy of different intensity levels and radial shock wave therapy for treating plantar fasciitis: a systematic review and network meta-analysis. Arch. Phys. Med. Rehabil. 93, 1259–1268.
Ciapetti, G., Ambrosio, L., Marletta, G., Baldini, N., Giunti, A., 2006. Human bone marrow stromal cells: in vitro expansion and differentiation for bone engineering. Biomaterials 27, 6150–6160.
English, K., French, A., Wood, K.J., 2010. Mesenchymal stromal cells: facilitators of successful transplantation? Cell Stem Cell 7, 431–442.
Faber-Elman, A., Solomon, A., Abraham, J.A., Marikovsky, M., Schwartz, M., 1996. Involvement of wound-associated factors in rat brain astrocyte migratory response to axonal injury: in vitro simulation. J. Clin. Invest. 97, 162–171.
Friedenstein, A.J., Piatetzky-Shapiro, I.I., Petrakova, K.V., 1966. Osteogenesis in transplants of bone marrow cells. J. Embryol. Exp. Morphol. 16, 381–390.
Friedenstein, A.J., Gorskaja, J.F., Kulagina, N.N., 1976. Fibroblast precursors in normal and irradiated mouse hematopoietic organs. Exp. Hematol. 4, 267–274.
Friedl, G., Schmidt, H., Rehak, I., Kostner, G., Schauenstein, K., Windhager, R., 2007. Undifferentiated human mesenchymal stem cells (hMSCs) are highly sensitive to mechanical strain: transcriptionally controlled early osteo-chondrogenic response in vitro. Osteoarthritis Cartilage 15, 1293–1300.
Ghanem, A., Steingen, C., Brenig, F., Funcke, F., Bai, Z.Y., Hall, C., Chin, C.T., Nickenig, G., Bloch, W., Tiemann, K., 2009. Focused ultrasound-induced stimulation of microbubbles augments site-targeted engraftment of mesenchymal stem cells after acute myocardial infarction. J. Mol. Cell. Cardiol. 47, 411–418.
Gnecchi, M., He, H., Liang, O.D., Melo, L.G., Morello, F., Mu, H., Noiseux, N., Zhang, L., Pratt, R.E., Ingwall, J.S., et al., 2005. Paracrine action accounts for marked protection of ischemic heart by Akt-modified mesenchymal stem cells. Nat. Med. 11, 367–368.
Haynesworth, S.E., Baber, M.A., Caplan, A.I., 1996. Cytokine expression by human marrow-derived mesenchymal progenitor cells in vitro: effects of dexamethasone and IL-1 alpha. J. Cell. Physiol. 166, 585–592.
Heidebrecht, H.J., Buck, F., Haas, K., Wacker, H.H., Parwaresch, R., 1996. Monoclonal antibodies Ki-S3 and Ki-S5 yield new data on the 'Ki-67' proteins. Cell Prolif. 29, 413–425.
Higuera, G., Schop, D., Janssen, F., van Dijkhuizen-Radersma, R., van Boxtel, T., van Blitterswijk, C.A., 2009. Quantifying in vitro growth and metabolism kinetics of human mesenchymal stem cells using a mathematical model. Tissue Eng. Part A 15, 2653–2663.
Hofmann, M., Wollert, K.C., Meyer, G.P., Menke, A., Arseniev, L., Hertenstein, B., Ganser, A., Knapp, W.H., Drexler, H., 2005. Monitoring of bone marrow cell homing into the infarcted human myocardium. Circulation 111, 2198–2202.
Ingber, D.E., 2006. Cellular mechanotransduction: putting all the pieces together again. FASEB J. 20, 811–827.
Jaalouk, D.E., Lammerding, J., 2009. Mechanotransduction gone awry. Nat. Rev. Mol. Cell Biol. 10, 63–73.
Jiang, Y., Jahagirdar, B.N., Reinhardt, R.L., Schwartz, R.E., Keene, C.D., Ortiz-Gonzalez, X.R., Reyes, M., Lenvik, T., Lund, T., Blackstad, M., et al., 2002. Pluripotency of mesenchymal stem cells derived from adult marrow. Nature 418, 41–49.
Karp, J.M., Leng Teo, G.S., 2009. Mesenchymal stem cell homing: the devil is in the details. Cell Stem Cell 4, 206–216.
Kasper, G., Glaeser, J.D., Geissler, S., Ode, A., Tuischer, J., Matziolis, G., Perka, C., Duda, G.N., 2007. Matrix metalloprotease activity is an essential link between mechanical stimulus and mesenchymal stem cell behavior. Stem Cells 25, 1985–1994.
Kato, M., Ioritani, N., Suzuki, T., Kambe, M., Inaba, Y., Watanabe, R., Sasano, H., Orikasa, S., 2000. Mechanism of anti-tumor effect of combination of bleomycin and shock waves. Jpn. J. Cancer Res. 91, 1065–1072.
Kearney, E.M., Prendergast, P.J., Campbell, V.A., 2008. Mechanisms of strain-mediated mesenchymal stem cell apoptosis. J. Biomech. Eng. 130, 061004.
Klotz, B., Mentrup, B., Regensburger, M., Zeck, S., Schneidereit, J., Schupp, N., Linden, C., Merz, C., Ebert, R., Jakob, F., 2012. 1,25-Dihydroxyvitamin D3 treatment delays cellular aging in human mesenchymal stem cells while maintaining their multipotent capacity. PLoS One 7, e29959.
Kolf, C.M., Cho, E., Tuan, R.S., 2007. Mesenchymal stromal cells. Biology of adult mesenchymal stem cells: regulation of niche, self-renewal and differentiation. Arthritis Res. Ther. 9, 204.
Krause, U., Harter, C., Seckinger, A., Wolf, D., Reinhard, A., Bea, F., Dengler, T., Hardt, S., Ho, A., Katus, H.A., et al., 2007. Intravenous delivery of autologous mesenchymal stem cells limits infarct size and improves left ventricular function in the infarcted porcine heart. Stem Cells Dev. 16, 31–37.
Kreis, T.E., Birchmeier, W., 1980. Stress fiber sarcomeres of fibroblasts are contractile. Cell 22, 555–561.
Kuznetsov, S.A., Friedenstein, A.J., Robey, P.G., 1997a. Factors required for bone marrow stromal fibroblast colony formation in vitro. Br. J. Haematol. 97, 561–570.
Kuznetsov, S.A., Krebsbach, P.H., Satomura, K., Kerr, J., Riminucci, M., Benayahu, D., Robey, P.G., 1997b. Single-colony derived strains of human marrow stromal fibroblasts form bone after transplantation in vivo. J. Bone Miner. Res. 12, 1335–1347.
Ladage, D., Brixius, K., Steingen, C., Mehlhorn, U., Schwinger, R.H., Bloch, W., Schmidt, A., 2007. Mesenchymal stem cells induce endothelial activation via paracine mechanisms. Endothelium 14, 53–63.
Li, L., Jiang, J., 2011. Regulatory factors of mesenchymal stem cell migration into injured tissues and their signal transduction mechanisms. Front. Med. 5, 33–39.
Mahmood, A., Lu, D., Lu, M., Chopp, M., 2003. Treatment of traumatic brain injury in adult rats with intravenous administration of human bone marrow stromal cells. Neurosurgery 53, 697–702.
Meinel, L., Karageorgiou, V., Hofmann, S., Fajardo, R., Snyder, B., Li, C., Zichner, L., Langer, R., Vunjak-Novakovic, G., Kaplan, D.L., 2004. Engineering bone-like tissue in vitro using human bone marrow stem cells and silk scaffolds. J. Biomed. Mater. Res. A 71, 25–34.
Mirotsou, M., Zhang, Z., Deb, A., Zhang, L., Gnecchi, M., Noiseux, N., Mu, H., Pachori, A., Dzau, V., 2007. Secreted frizzled related protein 2 (Sfrp2) is the key Akt-mesenchymal stem cell-released paracrine factor mediating myocardial survival and repair. Proc. Natl. Acad. Sci. U. S. A. 104, 1643–1648.
Morita, T., Kurihara, H., Maemura, K., Yoshizumi, M., Nagai, R., Yazaki, Y., 1994. Role of Ca^{2+} and protein kinase C in shear stress-induced actin depolymerization and endothelin 1 gene expression. Circ. Res. 75, 630–636.
Murphy, J.M., Fink, D.J., Hunziker, E.B., Barry, F.P., 2003. Stem cell therapy in a caprine model of osteoarthritis. Arthritis Rheum. 48, 3464–3474.
Nishida, T., Shimokawa, H., Oi, K., Tatewaki, H., Uwatoku, T., Abe, K., Matsumoto, Y., Kajihara, N., Eto, M., Matsuda, T., et al., 2004. Extracorporeal cardiac shock wave therapy markedly ameliorates ischemia-induced myocardial dysfunction in pigs in vivo. Circulation 110, 3055–3061.
Nombela-Arrieta, C., Ritz, J., Silberstein, L.E., 2011. The elusive nature and function of mesenchymal stem cells. Nat. Rev. Mol. Cell Biol. 12, 126–131.
Ode, A., Kopf, J., Kurtz, A., Schmidt-Bleek, K., Schrade, P., Kolar, P., Buttgereit, F., Lehmann, K., Hutmacher, D.W., Duda, G.N., et al., 2011. CD73 and CD29 concurrently mediate the

mechanically induced decrease of migratory capacity of mesenchymal stromal cells. Eur. Cell. Mater. 22, 26–42.
Okamoto, T., Aoyama, T., Nakayama, T., Nakamata, T., Hosaka, T., Nishijo, K., Nakamura, T., Kiyono, T., Toguchida, J., 2002. Clonal heterogeneity in differentiation potential of immortalized human mesenchymal stem cells. Biochem. Biophys. Res. Commun. 295, 354–361.
Patel, T., Gores, G.J., Kaufmann, S.H., 1996. The role of proteases during apoptosis. FASEB J. 10, 587–597.
Pellegrin, S., Mellor, H., 2007. Actin stress fibres. J. Cell Sci. 120, 3491–3499.
Peterson, K.M., Aly, A., Lerman, A., Lerman, L.O., Rodriguez-Porcel, M., 2011. Improved survival of mesenchymal stromal cell after hypoxia preconditioning: role of oxidative stress. Life Sci. 88, 65–73.
Pittenger, M.F., Mackay, A.M., Beck, S.C., Jaiswal, R.K., Douglas, R., Mosca, J.D., Moorman, M.A., Simonetti, D.W., Craig, S., Marshak, D.R., 1999. Multilineage potential of adult human mesenchymal stem cells. Science 284, 143–147.
Prockop, D.J., 2009. Repair of tissues by adult stem/progenitor cells (MSCs): controversies, myths, and changing paradigms. Mol. Ther. 17, 939–946.
Rid, R., Schiefermeier, N., Grigoriev, I., Small, J.V., Kaverina, I., 2005. The last but not the least: the origin and significance of trailing adhesions in fibroblastic cells. Cell Motil. Cytoskeleton 61, 161–171.
Sacchetti, B., Funari, A., Michienzi, S., Di, C.S., Piersanti, S., Saggio, I., Tagliafico, E., Ferrari, S., Robey, P.G., Riminucci, M., et al., 2007. Self-renewing osteoprogenitors in bone marrow sinusoids can organize a hematopoietic microenvironment. Cell 131, 324–336.
Schmidt, A., Ladage, D., Schinkothe, T., Klausmann, U., Ulrichs, C., Klinz, F.J., Brixius, K., Arnhold, S., Desai, B., Mehlhorn, U., et al., 2006. Basic fibroblast growth factor controls migration in human mesenchymal stem cells. Stem Cells 24, 1750–1758.
Scholzen, T., Gerdes, J., 2000. The Ki-67 protein: from the known and the unknown. J. Cell. Physiol. 182, 311–322.
Schumann, D., Kujat, R., Zellner, J., Angele, M.K., Nerlich, M., Mayr, E., Angele, P., 2006. Treatment of human mesenchymal stem cells with pulsed low intensity ultrasound enhances the chondrogenic phenotype in vitro. Biorheology 43, 431–443.
Song, L., Webb, N.E., Song, Y., Tuan, R.S., 2006. Identification and functional analysis of candidate genes regulating mesenchymal stem cell self-renewal and multipotency. Stem Cells 24, 1707–1718.
Spallarossa, P., Altieri, P., Barisione, C., Passalacqua, M., Aloi, C., Fugazza, G., Frassoni, F., Podesta, M., Canepa, M., Ghigliotti, G., et al., 2010. p38 MAPK and JNK antagonistically control senescence and cytoplasmic p16INK4A expression in doxorubicin-treated endothelial progenitor cells. PLoS One 5, e15583.
Steingen, C., 2008. Characterization of key mechanisms involved in transmigration and invasion of mesenchymal stem cells. PhD thesis, University of Cologne.
Steingen, C., Brenig, F., Baumgartner, L., Schmidt, J., Schmidt, A., Bloch, W., 2008. Characterization of key mechanisms in transmigration and invasion of mesenchymal stem cells. J. Mol. Cell. Cardiol. 44, 1072–1084.
Tondreau, T., Lagneaux, L., Dejeneffe, M., Massy, M., Mortier, C., Delforge, A., Bron, D., 2004. Bone marrow-derived mesenchymal stem cells already express specific neural proteins before any differentiation. Differentiation 72, 319–326.
Traut, W., Scholzen, T., Winking, H., Kubbutat, M.H., Gerdes, J., 1998. Assignment1 of the murine Ki-67 gene (Mki67) to chromosome band 7F3–F5 by in situ hybridization. Cytogenet. Cell Genet. 83, 12–13.
van der Jagt, O.P., Piscaer, T.M., Schaden, W., Li, J., Kops, N., Jahr, H., van der Linden, J.C., Waarsing, J.H., Verhaar, J.A., de Jong, M., et al., 2011. Unfocused extracorporeal shock waves induce anabolic effects in rat bone. J. Bone Joint Surg. Am. 93, 38–48.
van der Jagt, O.P., Waarsing, J.H., Kops, N., Schaden, W., Jahr, H., Verhaar, J.A., Weinans, H., 2013. Unfocused extracorporeal shock waves induce anabolic effects in osteoporotic rats. J. Orthop. Res. 31, 768–775.
Wang, C.J., Wang, F.S., Yang, K.D., Weng, L.H., Hsu, C.C., Huang, C.S., Yang, L.C., 2003. Shock wave therapy induces neovascularization at the tendon–bone junction. A study in rabbits. J. Orthop. Res. 21, 984–989.
Wolf, D., Reinhard, A., Seckinger, A., Katus, H.A., Kuecherer, H., Hansen, A., 2009. Dose-dependent effects of intravenous allogeneic mesenchymal stem cells in the infarcted porcine heart. Stem Cells Dev. 18, 321–329.
Yan, S.G., Huang, L.Y., Cai, X.Z., 2011. Low-intensity pulsed ultrasound: a potential non-invasive therapy for femoral head osteonecrosis. Med. Hypotheses 76, 4–7.
Yeh, K.H., Sheu, J.J., Lin, Y.C., Sun, C.K., Chang, L.T., Kao, Y.H., Yen, C.H., Shao, P.L., Tsai, T.H., Chen, Y.L., et al., 2012. Benefit of combined extracorporeal shock wave and bone marrow-derived endothelial progenitor cells in protection against critical limb ischemia in rats. Crit. Care Med. 40, 169–177.
Zaragosi, L.E., Ailhaud, G., Dani, C., 2006. Autocrine fibroblast growth factor 2 signaling is critical for self-renewal of human multipotent adipose-derived stem cells. Stem Cells 24, 2412–2419.